Journal of Biomechanics 46 (2013) 780–787

Contents lists available at SciVerse ScienceDirect

Journal of Biomechanics

journal homepage: www.elsevier.com/locate/jbiomech
www.JBiomech.com

Muscle contributions to fore-aft and vertical body mass center accelerations over a range of running speeds

Samuel R. Hamner [a], Scott L. Delp [a,b,*]

[a] Department of Mechanical Engineering, Stanford University, USA
[b] Department of Bioengineering, Stanford University, USA

ARTICLE INFO

Article history:
Accepted 6 November 2012

Keywords:
Running biomechanics
Human locomotion
Forward dynamic simulation
Muscle function
Musculoskeletal modeling
Induced acceleration analysis

ABSTRACT

Running is a bouncing gait in which the body mass center slows and lowers during the first half of the stance phase; the mass center is then accelerated forward and upward into flight during the second half of the stance phase. Muscle-driven simulations can be analyzed to determine how muscle forces accelerate the body mass center. However, muscle-driven simulations of running at different speeds have not been previously developed, and it remains unclear how muscle forces modulate mass center accelerations at different running speeds. Thus, to examine how muscles generate accelerations of the body mass center, we created three-dimensional muscle-driven simulations of ten subjects running at 2.0, 3.0, 4.0, and 5.0 m/s. An induced acceleration analysis determined the contribution of each muscle to mass center accelerations. Our simulations included arms, allowing us to investigate the contributions of arm motion to running dynamics. Analysis of the simulations revealed that soleus provides the greatest upward mass center acceleration at all running speeds; soleus generates a peak upward acceleration of 19.8 m/s^2 (i.e., the equivalent of approximately 2.0 bodyweights of ground reaction force) at 5.0 m/s. Soleus also provided the greatest contribution to forward mass center acceleration, which increased from 2.5 m/s^2 at 2.0 m/s to 4.0 m/s^2 at 5.0 m/s. At faster running speeds, greater velocity of the legs produced larger angular momentum about the vertical axis passing through the body mass center; angular momentum about this vertical axis from arm swing simultaneously increased to counterbalance the legs. We provide open-access to data and simulations from this study for further analysis in OpenSim at simtk.org/home/nmbl_running, enabling muscle actions during running to be studied in unprecedented detail.

1. Introduction

As runners increase their speed, the magnitude of forces acting on their bodies increases. Researchers have observed changes in ground reaction forces, joint moments, muscle activities, leg stiffness, and body segment motions at different running speeds (e.g., Cappellini et al., 2006; Cavagna et al., 1976; McClay et al., 1990; McMahon and Cheng, 1990; Novacheck, 1998; Schache et al., 2011; Winter, 1983). Analysis of body segment motions and ground reaction forces during running has revealed that runners increase their forward speed by increasing their stride length and stride frequency (Cavagna et al., 1988; Hildebrand, 1960). At running speeds between 2 and 7 m/s, runners increase their stride length by generating larger ground reaction forces (Derrick et al., 1998; Mercer et al., 2005; Weyand et al., 2000). These experimental studies have characterized the larger ground reaction forces runners produce as they run faster, yet it remains unclear which muscles contribute to the production of larger ground reaction forces as running speed increases.

Musculoskeletal simulations enable examination of how muscles produce ground reaction forces. Muscles generate forces that are transmitted by bones and connective tissue to other body segments, causing the foot to apply a force to the ground. The ground applies an equal and opposite reaction force to each foot, which accelerates the mass center forward (i.e., propulsion), backward (i.e., braking), and upward (i.e., support). The mass center acceleration is equal to the ground reaction force divided by the subject's total body mass (Winter, 1990). Sasaki and Neptune (2006) used two-dimensional simulations to highlight a change in soleus function at the walk-run transition speed. Besier et al. (2009) estimated muscle forces during running with an electromyography-driven musculoskeletal model to characterize quadriceps forces in subjects with patellafemoral pain. Dorn et al. (2012) estimated muscle forces during running and sprinting using static optimization, and calculated muscle contributions

* Correspondence to: Clark Center, Room S-321, Stanford University, Mail Code 5450, 318 Campus Drive, Stanford, CA 94305-5450, USA. Tel.: +1 650 723 1230; fax: +1 650 723 8544.
E-mail address: delp@stanford.edu (S.L. Delp).

0021-9290/$ - see front matter © 2012 Elsevier Ltd. All rights reserved.
http://dx.doi.org/10.1016/j.jbiomech.2012.11.024

to vertical mass center and hip accelerations. However, static optimization excludes effects of activation dynamics and tendon compliance on muscle force production. Achilles tendon compliance decreases metabolic cost during running (Alexander and Bennet-Clark, 1977) and affects muscle fiber lengths, fiber velocities, and force generation during running (Biewener and Roberts, 2000; Farris and Sawicki, 2012).

We previously developed a three-dimensional muscle-driven simulation of a single subject running at approximately 4 m/s that included activation dynamics and tendon compliance (Hamner et al., 2010). Analysis of the simulation revealed that quadriceps and plantarflexors are major contributors to mass center acceleration at this running speed. We observed that arm motion effectively counterbalanced angular momentum about the vertical axis passing through the body mass center from leg swing, but had little effect on mass center accelerations. In this study, we extend upon our previous work by developing and analyzing muscle-driven simulations of multiple subjects running over a range of speeds.

Our goal was to examine how muscle forces and arm swing affect dynamics of the body at different running speeds. Specifically, we sought to determine how muscle forces contribute to mass center accelerations during the stance phase of running, and how the arms act to counterbalance motion of the legs at different running speeds. We achieved this goal by creating and analyzing muscle-driven dynamic simulations of ten subjects running at different speeds. As the simulations are based on experimental data, we also report measured joint angles, joint moments, and ground reaction forces that occurred during running at different speeds.

2. Methods

We measured motions, forces, and electromyography (EMG) patterns of ten subjects running on a treadmill at four speeds: 2.0, 3.0, 4.0, and 5.0 m/s and used these data to create muscle-driven simulations of each subject at each speed. The simulations were analyzed to determine muscle contributions to vertical, backward, and forward mass center accelerations during the stance phase. Subjects were all male with an average age, height, and mass of 29 ± 5 years, 1.77 ± 0.04 m, and 70.9 ± 7.0 kg, respectively. Each subject was an experienced long distance runner who reported running at least 50 km/week. Seven subjects were consistent mid-to-rearfoot strikers and three subjects were consistent forefoot strikers at all running speeds examined in this study, except one forefoot striking subject who landed on his rearfoot while running at 2 m/s. The Stanford University Institutional Review Board approved the experimental protocol and subjects provided informed consent to participate.

2.1. Experimental data

Marker trajectories and ground reaction forces and moments were collected as each subject ran on a treadmill at different speeds. We placed 54 reflective markers on each subject and collected a static calibration trial. Functional joint movements were measured to calculate hip joint centers (Gamage and Lasenby, 2002). Marker positions were measured at 100 Hz using eight Vicon MX40+ cameras. Ground reaction forces and moments were measured at 1000 Hz using a Bertec Corporation instrumented treadmill. Marker positions and ground reaction forces were low pass filtered at 15 Hz with a zero-phase 4th order Butterworth filter and critically damped filter (Robertson and Dowling, 2003), respectively.

EMG signals were recorded using a Delsys Bangoli System with surface electrodes placed on 10 muscles: soleus, gastrocnemius lateralis, gastrocnemius medialis, tibialis anterior, biceps femoris long head, vastus medialis, vastus lateralis, rectus femoris, gluteus maximus, and gluteus medius. The raw EMG signal from each muscle was corrected for offset, rectified, and low-pass filtered at 10 Hz with a zero-phase 2nd order Butterworth filter (Buchanan et al., 2005). We then normalized the processed EMG signal from each muscle by the maximum voltage recorded across all trials for each subject.

2.2. Musculoskeletal simulations

Musculoskeletal simulations were generated using OpenSim (Delp et al., 2007). A 12 segment, 29 degree-of-freedom generic musculoskeletal model (Hamner et al., 2010) was used to create the simulations (Fig. 1; Supplemental Movie 1). Lower extremity and back joints were driven by 92 Hill-type musculotendon actuators (Anderson and Pandy, 1999; Delp et al., 1990) and arms were driven by torque actuators. We scaled the generic model to match each subject's anthropometry based on experimentally measured markers placed on anatomical landmarks and calculated hip joint centers. A virtual marker set was placed on the model based on these anatomical landmarks. Joint angles were calculated using an inverse kinematics algorithm that minimized the difference between experimentally measured marker positions and corresponding virtual markers on the model at each time frame. Joint moments were calculated using the residual reduction algorithm (RRA) (Delp et al., 2007). RRA allows for small changes in joint angles (RMS change $< 1.5^\circ$) and torso mass center location (RMS change < 5 cm) to minimize residual forces and moments applied to the pelvis (Kuo, 1998). Muscle excitations, activations, and forces needed to generate those moments and track the measured motion were estimated with the computed muscle control (CMC) algorithm (Thelen and Anderson, 2006; Thelen et al., 2003). CMC estimates muscle forces by minimizing the sum of the square of muscle excitations while accounting for muscle activation and contraction dynamics (Zajac, 1989). Constraints were applied to the muscle excitations for gluteus medius, semimembranosus, biceps femoris long head, vastus lateralis, gastrocnemius medialis, gastrocnemius lateralis, soleus, and tibialis anterior so that they better matched EMG recordings.

Supplementary material related to this article can be found online at http://dx.doi.org/10.1016/j.jbiomech.2012.11.024.

To test the accuracy of the simulations, we compared simulated quantities to experimental data. The simulations tracked measured kinematics with a maximum RMS deviation of 2.5° for each joint angle over a gait cycle. Simulated muscle activations and experimental EMG data showed similar features (Fig. 2), including strong activation during the stance phase of soleus, gastrocnemius medialis, gastrocnemius lateralis, vasti lateralis, vasti medialis, biceps femoris long head, gluteus maximus, and gluteus medius. There was a delay of approximately

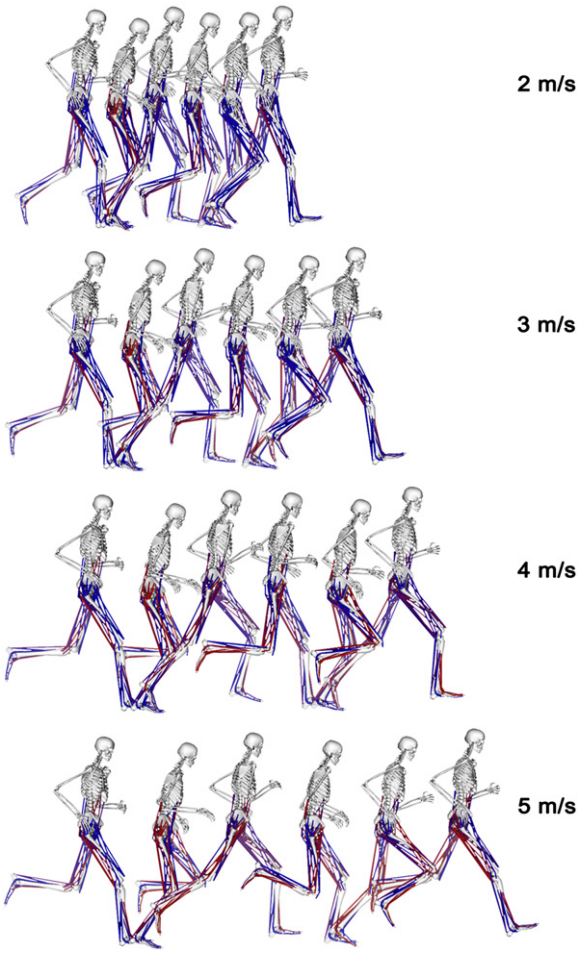

Fig. 1. Musculoskeletal model used to generate simulations of the running gait cycle for ten subjects at four running speeds: 2.0, 3.0, 4.0, and 5.0 m/s. Snapshots from the simulations of a representative subject illustrate a complete gait cycle at each speed. The gait cycle starts at right foot strike and ends at the subsequent right foot strike. Muscle color indicates simulated activation level from no activation (dark blue) to full activation (bright red).

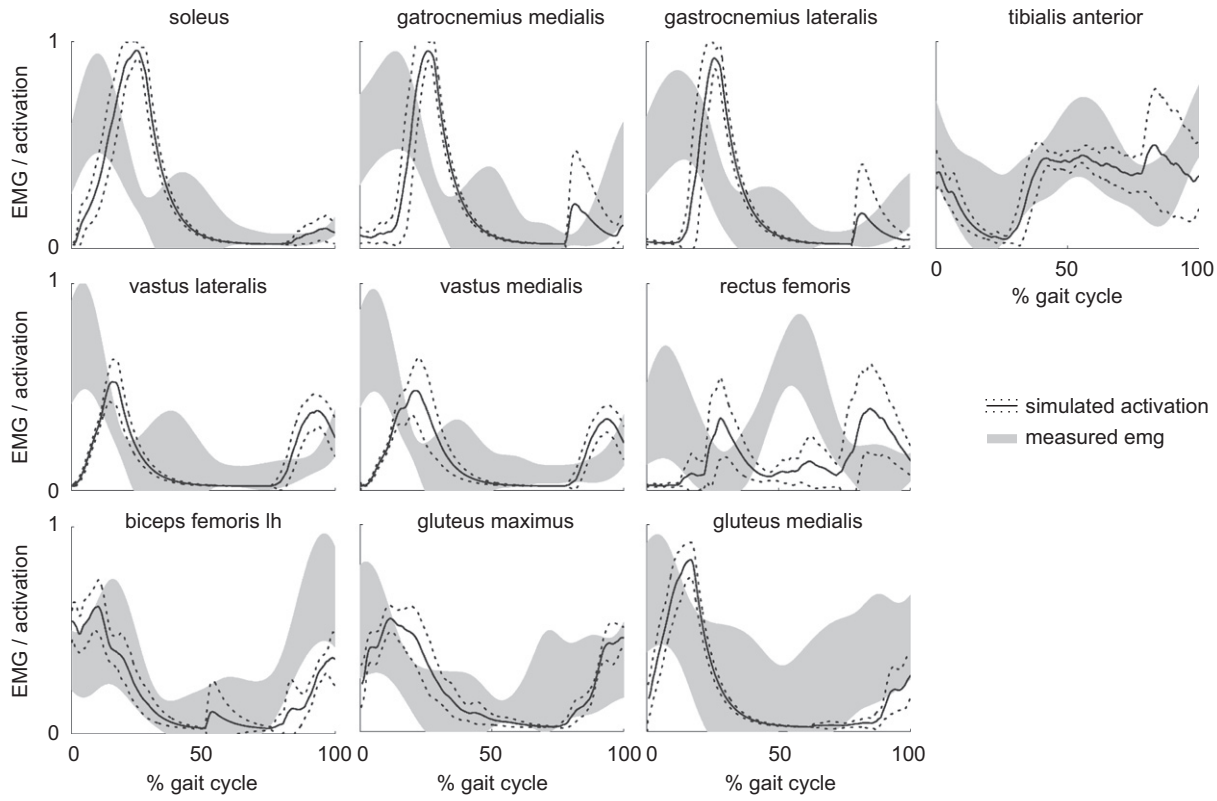

Fig. 2. Average simulated muscle activations from computed muscle control (solid black line; dashed line represents ± 1 standard deviation) and average experimental EMG (gray area) collected with surface electrodes from ten subjects running at 5.0 m/s. Data represents the average of three gait cycles for all ten subjects (i.e., a total of 30 gait cycles). See Supplemental Figs. 6–8 for other running speeds. EMG data of each muscle was normalized for each subject to the maximum processed signal for all data collected for that subject and the gray area represents the mean ± 1 standard deviation. Simulated activations are defined to be between 0 (no activation) and 1 (full activation).

75 ms between the processed EMG and simulated activations, consistent with electromechanical delay observed between measured EMG and force production (Corcos et al., 1992). Joint angles from inverse kinematics, joint moments from RRA, and experimentally measured ground reaction forces were compared to averaged data from previous studies (Cavanagh and Lafortune, 1980; Novacheck, 1998; Schache et al., 2011; Swanson and Caldwell, 2000; Winter, 1983) (Supplemental Fig. 1). Simulated muscle forces were compared to results from a static optimization study (Dorn et al., 2012) (Supplemental Fig. 2). The peak residual forces applied to the simulations were less than 2% of body weight and the peak residual and reserve moments applied to each joint were less than 0.05 Nm/kg (Supplemental Fig. 3).

An induced acceleration analysis was used to determine the contribution of each muscle force to vertical and fore-aft mass center accelerations. Each force in the simulation, including muscle forces, gravity, and forces due to velocity effects, was applied in isolation to calculate its contribution to the ground reaction force and mass center acceleration. Foot–floor interaction was modeled with a rolling without slipping constraint (Hamner et al., 2010). To test the accuracy of the analysis, we verified that the sum of accelerations due to each force reasonably matched the measured total mass center acceleration (Supplemental Fig. 4).

2.3. Statistics

Data were averaged across three right-foot stance phases for each subject at each running speed. Stance phase was normalized (from 0 to 100%) starting at foot strike and ending at toe-off determined from the measured vertical ground reaction force. Peak total mass center acceleration and muscle contributions to vertical, backward, and forward accelerations were averaged across all subjects for each speed. To determine if running speed had an effect on muscle contributions to mass center accelerations we performed a one-way repeated measures ANOVA for each muscle. One-way repeated measures ANOVA were also performed to determine if running speed had an effect on peak sagittal joint angles, peak sagittal joint moments, peak ground reaction forces, stride length, and the timing of gait events (i.e., toe-off, stride time, stance time, and flight time). We also performed the Shapiro–Wilk test with a significance level of 0.05 to ensure the data were normally distributed before performing the ANOVA. Effects of running speed were considered significant when $p < 0.01$.

3. Results

Peak sagittal joint angles, sagittal joint moments, and ground reaction forces significantly increased with running speed. Peak hip flexion, knee flexion, and ankle plantarflexion each increased due to running speed, with increases of 24°, 43°, and 10°, respectively, from 2.0 m/s to 5.0 m/s (Fig. 3A). Peak joint moments generated by the hip extensors, knee extensors, and ankle plantarflexors also increased due to running speed, with increases of 117%, 54%, and 35%, respectively, from 2.0 m/s to 5.0 m/s (Fig. 3B). Peak knee extension and ankle plantarflexion moments occurred near mid-stance, whereas the peak hip extension moment occurred during late swing at all speeds.

Duration of the stance phase decreased by 0.11 s across running speeds and toe-off took place earlier in the gait cycle at faster running speeds (Table 1). During the first half of the stance phase, the mass center accelerated backward (i.e., braking phase), and during the second half of stance the mass center accelerated forward (i.e., propulsion phase) (Fig. 4A). Running speed had a significant effect on peak backward, forward, and upward mass center accelerations. Peak forward ground reaction force increased from 0.13 bodyweights at 2.0 m/s to 0.34 bodyweights at 5.0 m/s, as vertical ground reaction force increased from 2.1 bodyweights at 2.0 m/s to 2.6 bodyweights at 5.0 m/s (Fig. 3C). Peak vertical ground reaction force occurred at 40% of the stance phase for 2.0 m/s and at 48% of stance for 5.0 m/s (Fig. 3C, vertical force).

Soleus was the largest contributor to upward mass center acceleration (Fig. 5A); with a peak contribution at 5.0 m/s that was 77% of total peak upward acceleration. The large upward mass center acceleration from soleus arose because the muscle force produced a large vertical ground reaction force of

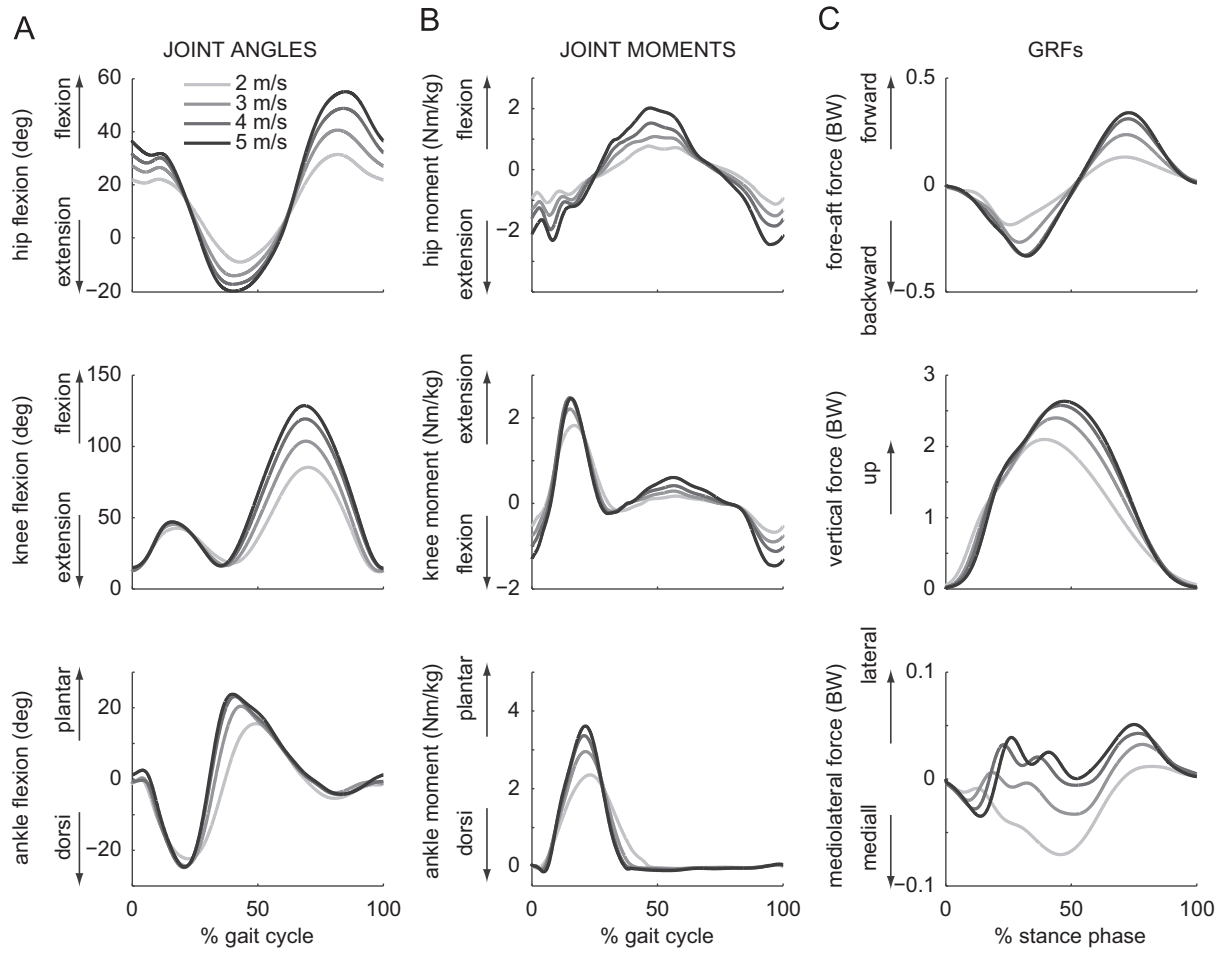

Fig. 3. (**A**) Joint angles from inverse kinematics for the sagittal hip, knee, and ankle averaged across subjects over the gait cycle, (**B**) joint moments from the residual reduction algorithm (RRA) for the sagittal hip, knee, and ankle averaged across subjects over the gait cycle, and (**C**) ground reaction forces averaged across subjects over the stance phase. Each plot includes data of four running speeds: 2.0, 3.0, 4.0, and 5.0 m/s.

Table 1
Average and standard deviation of toe-off, which is the instant in the gait cycle when the foot loses contact with ground; stride length, which is the distance traveled during a gait cycle; stride time, which is the duration of a gait cycle; stance time, which is the duration of the stance phase; and flight time, which is the duration of the flight phase (i.e., period when both feet are off the ground). A one-way, repeated measures ANOVA indicated that speed had a significant effect ($^*p < 0.01$) on each of these quantities.

Speed (m/s)	**Toe-off* (% GC)** mean (SD)	**Stride Length* (m)** mean (SD)	**Stride Time* (s)** mean (SD)	**Stance Time* (s)** mean (SD)	**Flight Time* (s)** mean (SD)
2.0	46.7 (2.5)	1.50 (0.08)	0.752 (0.041)	0.343 (0.019)	0.038 (0.021)
3.0	40.4 (2.2)	2.14 (0.10)	0.715 (0.032)	0.289 (0.022)	0.068 (0.014)
4.0	38.3 (2.7)	2.69 (0.11)	0.672 (0.027)	0.258 (0.025)	0.081 (0.016)
5.0	37.5 (1.8)	3.00 (0.37)	0.619 (0.029)	0.236 (0.020)	0.077 (0.017)

approximately 2 bodyweights. Peak contributions from soleus to upward mass center acceleration increased by 5.7 m/s^2 across running speeds (Fig. 5A). Gastrocnemius, vasti, and gluteus maximus also contributed substantially to upward acceleration. Contributions of vasti (Fig. 4E) and gluteus maximus (Fig. 4G) to upward mass center acceleration peaked during the braking phase, whereas contribution of plantarflexors (Fig. 4C & D) to upward acceleration peaked during the propulsion phase. In contrast, tibialis anterior and the hamstrings contribute to a downward acceleration during stance (Fig. 4H & I) by providing ankle dorsiflexion and knee flexion moments, respectively.

During the braking phase, the quadriceps muscle group (i.e., vasti and rectus femoris) produced a large backward mass center acceleration (Fig. 5B); at 5.0 m/s, peak contribution from quadriceps was 80% of total peak backward acceleration. This large backward mass center acceleration from quadriceps arose because the muscle forces produced a backward ground reaction force of approximately 0.3 bodyweights. Contributions from vasti to backward mass center acceleration increased by 0.7 m/s^2 across running speeds (Fig. 5B). Tibialis anterior contributed about 20% of peak backward acceleration, and did not significantly change with running speed.

During the propulsion phase, the ankle plantarflexors (i.e., gastrocnemius and soleus) were the largest contributors to forward mass center acceleration (Fig. 5B), with a peak forward acceleration at 5.0 m/s that was larger than the total peak forward mass center acceleration. The contribution from plantarflexors to forward acceleration was greater than the total forward mass center acceleration because quadriceps continued to accelerate

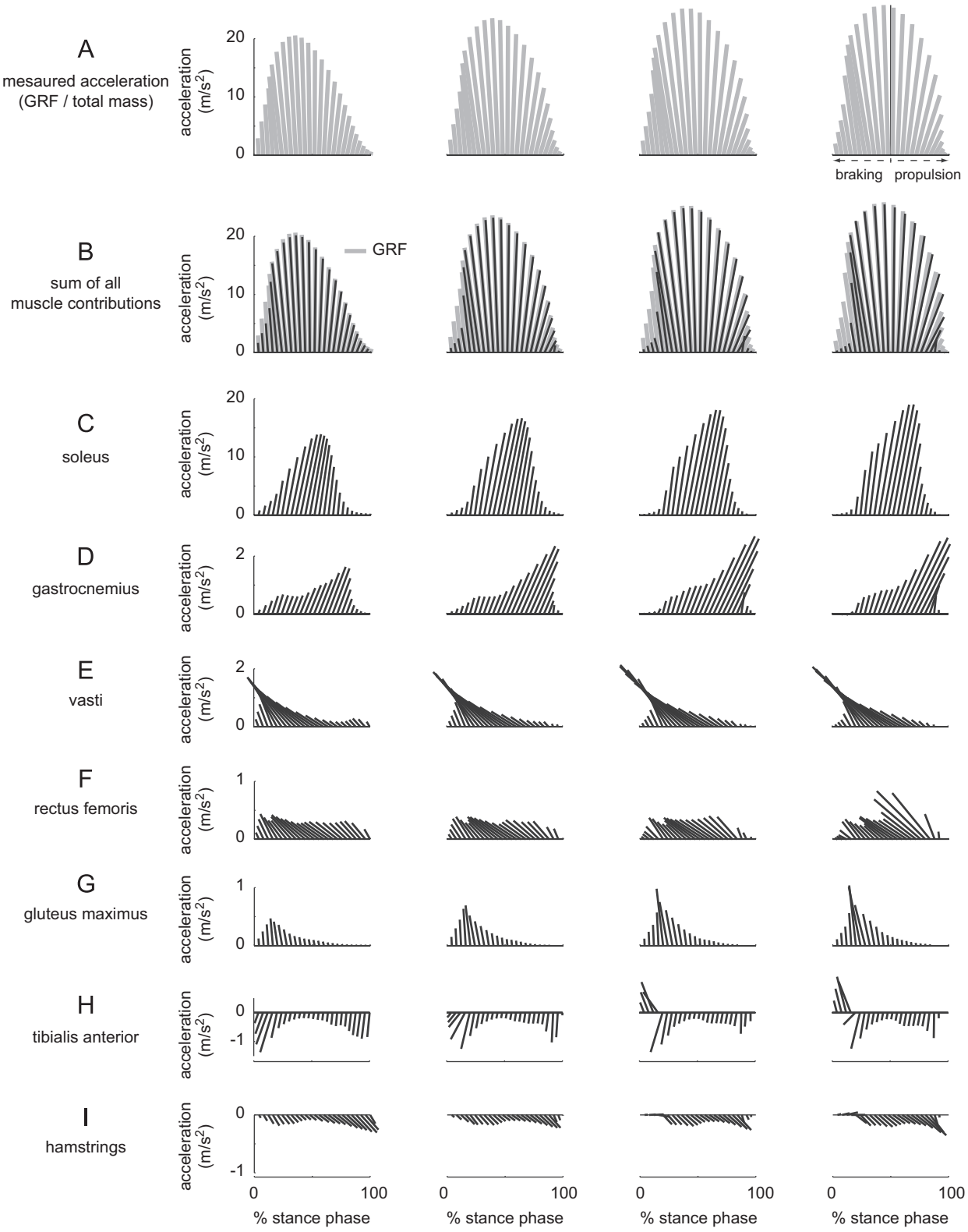

Fig. 4. Muscle contributions to the body mass center acceleration during stance, across a range of running speeds. Each ray is the resultant vector of contributions to fore-aft acceleration (i.e., propulsion and braking) and vertical acceleration (i.e., support), averaged across ten subjects. (**A**) Total mass center acceleration as calculated by dividing the measured ground reaction force by each subject's total body mass. (**B**) The sum of all muscle contributions is compared to the measured mass center acceleration to illustrate the accuracy of the analysis. Notice the scale for soleus (**C**) is greater than any other muscle (**D**-**I**), as soleus was the largest contributor to upward and forward mass center acceleration.

the mass center backward during the propulsion phase. Peak contributions from soleus to forward mass center acceleration increased by 1.4 m/s^2 across running speeds (Fig. 5B). The contribution from gastrocnemius at 5.0 m/s was 35% of the peak forward acceleration, and increased by 0.7 m/s^2 across speeds (Fig. 5B). Hamstrings and forces due to velocity effects

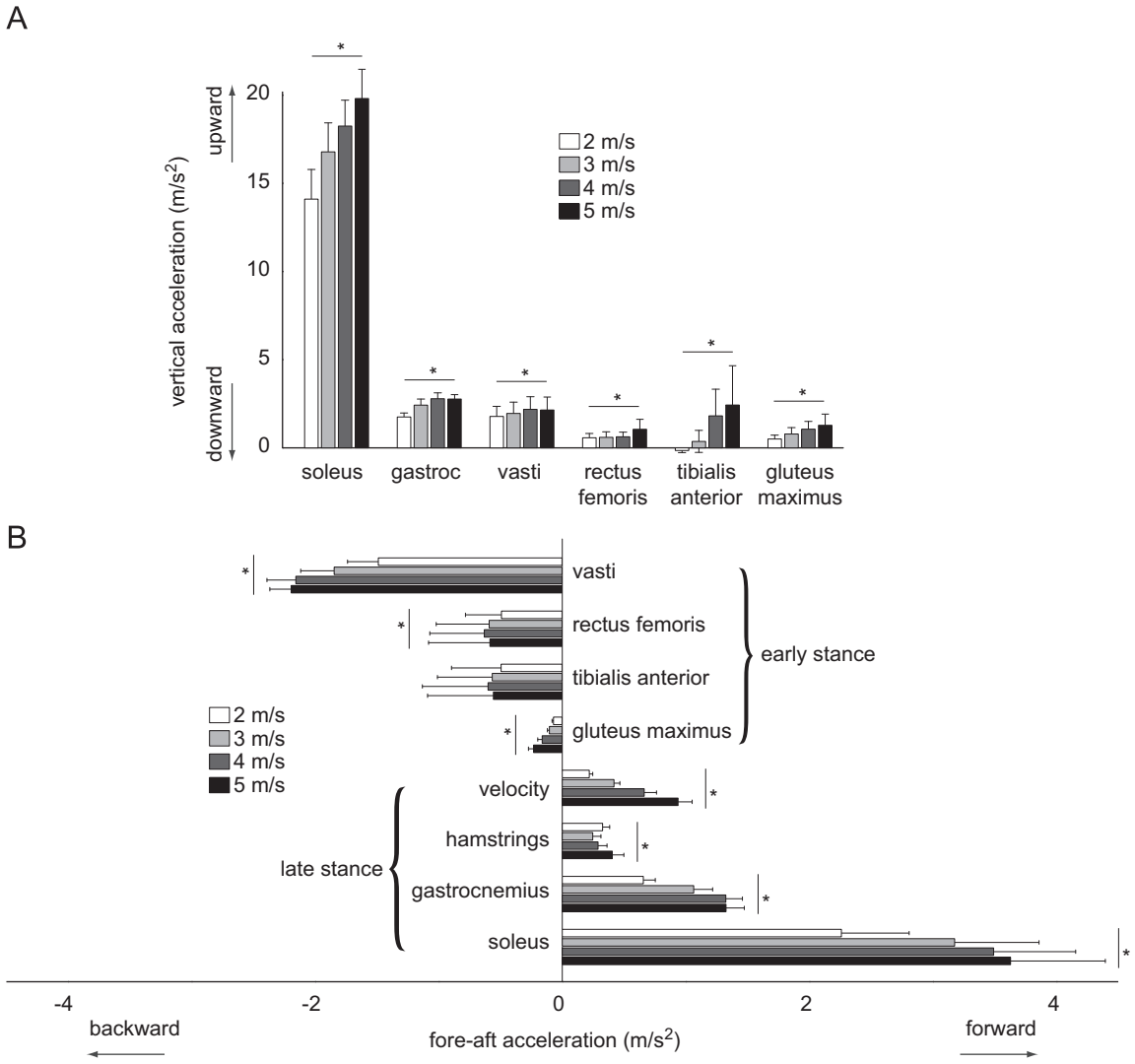

Fig. 5. Peak contributions to (**A**) upward acceleration (i.e., support) and (**B**) fore-aft accelerations (i.e., braking and propulsion) from muscles and forces due to velocity effects (i.e., Coriolis and centripetal forces), averaged over ten subjects. Peak contributions to backward acceleration occurred during early stance while peak forward accelerations occurred during late stance. Error bars span $\pm$ one standard deviation. A repeated measures ANOVA indicated that speed had a significant effect ($^*p < 0.01$) on muscle contributions mass center acceleration from soleus, gastrocnemius, vasti, rectus femoris, gluteus maximus, and tibialis anterior.

(i.e., Corriolis and centripetal forces) also contributed to forward mass center acceleration and each showed a significant change with speed.

While arms contributed little to mass center accelerations, we also observed that angular momentum of the arms about a vertical axis passing through the center of mass counterbalanced (i.e., was equal and opposite to) angular momentum of the lower extremities (Fig. 6). Running speed had a significant effect on peak vertical angular momentum of the arms and legs, each of which doubled, from about 1.5 kg-m^2/s at 2.0 m/s to 3.0 kg-m^2/s at 5.0 m/s.

4. Discussion

Our goal was to determine how muscle forces and arm swing affect dynamics of the body at different running speeds. Our analysis revealed that upward, backward, and forward mass center accelerations were generated primarily by muscles of the stance limb. During the early stance phase of the running gait cycle, the quadriceps muscle group was the largest contributor to backward and upward mass center acceleration at each speed. During late stance, the ankle plantarflexors (i.e., soleus and gastrocnemius) were the main contributors to forward and upward mass center accelerations. We observed that running speed had a significant effect on upward and fore-aft mass center accelerations produced by soleus, gastrocnemius, vasti, rectus femoris, hamstrings, gluteus maximus, and gluteus medius.

Soleus was the dominant contributor to upward and forward mass center accelerations at all running speeds. Large mass center accelerations from soleus occur because the muscle produces a large force and is a uniarticular ankle plantarflexor. Gastrocnemius, the other major ankle plantarflexor, also crosses the knee and generates a knee flexion moment, which reduces its capacity to accelerate the mass center upwards. Increased contributions to upward and forward mass center accelerations by soleus enable longer flight times and larger stride lengths (Table 1), providing a means of increasing running speed (Dorn et al., 2012; Weyand et al., 2000). Thus, soleus plays an important role in increasing forward running speed from 2–5 m/s by generating larger upward and forward mass center accelerations.

At the fastest running speed in this study (5.0 m/s), soleus muscle fibers shortened with the highest velocities of any muscle in the simulation during late stance (Supplemental Fig. 5), which

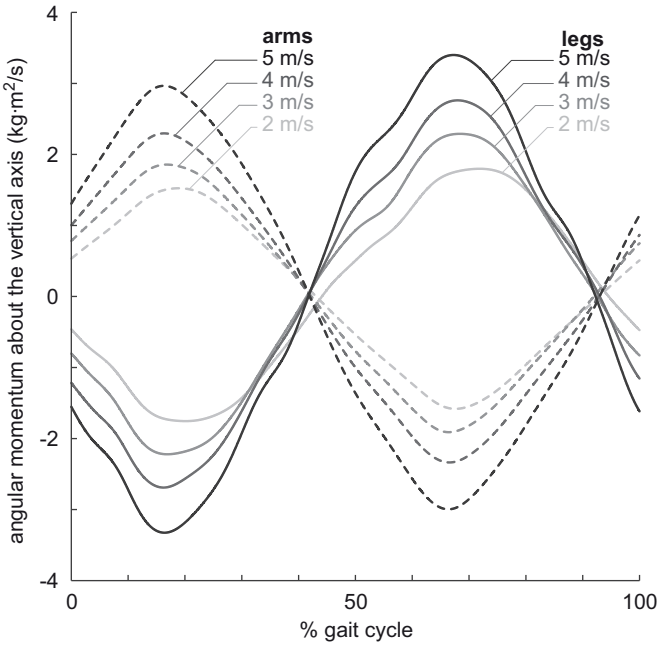

Fig. 6. The angular momentum of the arms (dashed lines) and legs (solid lines) computed about the vertical axis passing through the body mass center during the running gait cycle of ten subjects at four running speeds (2.0, 3.0, 4.0, and 5.0 m/s) averaged for ten subjects. The vertical angular momentum was calculated for all body segments. The arms consisted of the humerus, ulna, radius and hand segments, and the legs consisted of the femur, tibia, and foot segments. The vertical angular momentum of the arms was nearly equal and opposite that of the legs at each running speed.

corresponds with increased excursion of the ankle (Fig. 3A) and decreased ground contact time (Table 1). Diminishing force production due to high fiber velocities has been suggested as a mechanism that limits running speed (Dorn et al., 2012; Miller et al., 2012a). Since runners generate larger upward and forward mass center accelerations at faster running speeds (Schache et al., 2012; Weyand et al., 2000), and soleus is the largest contributor to these accelerations, limited force production from soleus due to its high shortening velocity may therefore limit a runner's speed. Muscle fiber length and velocity are sensitive to tendon compliance (Biewener and Roberts, 2000) and parameters of the force–velocity relationship, such as maximum fiber contractile velocity and shape of the force–velocity curve (Miller et al., 2012b). Our work did not formally characterize sensitivity of soleus force to these parameters but we expect that force production by soleus to be particularly sensitive to fiber velocity since this muscle has a high fraction of slow twitch muscle fibers (Edgerton et al., 1975). Future research of running performance should characterize the relationship between muscle parameters and soleus force production and compare simulation results with imaging studies (e.g., Farris and Sawicki, 2012; Lichtwark et al., 2007) to verify fiber lengths and velocities.

To assess the accuracy of the simulations and gain confidence in the analysis results from this study, we compared our simulated results to results from experimental studies that have measured joint moments and muscle activity over a range of running speeds. Average hip flexion, knee extension, and ankle plantarflexion moments generated by muscle forces showed similar features to data from Schache et al. (2011), demonstrating a significant increase in ankle plantarflexion moment with increased running speed. Muscle activity from our simulations also showed similar features to EMG collected by Cappellini et al. (2006), including increased activations of the quadriceps during early stance and increased activation of the plantarflexors during mid-to-late stance. These observed increases in joint moments and muscle activity support our finding of increased contributions from the quadriceps to backward and upward mass center accelerations during early stance and increased contributions from the plantarflexors to forward and upward accelerations during late stance.

Our previous simulation of running (Hamner et al., 2010) also showed that soleus and gastrocnemius are large contributors to upward and forward mass center accelerations. However, contributions from vasti to upward and backward accelerations in this study are less than our previous results. The previous simulation was of one stride from a single subject running at a single speed. During that stride, the subject decelerated over the stance phase (i.e., the braking impulse was greater than the propulsive impulse) and generated a larger knee extension moment compared to average moments from this study. These differences may have required a larger contribution from quadriceps in our previous simulation. Our current study includes ten subjects running at four speeds with three strides at each speed, for a total of 120 simulations. This larger set of data likely provides a more accurate assessment of quadriceps actions.

We found that arms made negligible contributions to mass center accelerations at the running speeds we studied, although arms may make larger contributions to forward and vertical accelerations at faster running speeds. As previously observed, we found that the arms counterbalanced the vertical angular momentum of the legs (Hamner et al., 2010; Hinrichs et al., 1987), which may help to minimize rotation of the head and torso (Pontzer et al., 2009).

This study was performed using an instrumented treadmill that measures ground reaction forces. Slight differences have been observed in kinematics, kinetics, and EMG between over ground and treadmill running (Nigg et al., 1995; Wank et al., 1998). However, motions and ground reaction forces from treadmill running in this study are consistent with data from over ground studies (Cavanagh and Lafortune, 1980; Novacheck, 1998; Schache et al., 2011; Winter, 1983) (Supplemental Fig. 1). Nigg et al. (1995) observed less difference in kinematics and kinetics of experienced runners between over ground and treadmill running, and this study examined only experienced runners. Additionally, we observed that muscle forces calculated in this study are consistent with Dorn et al. (2012), who calculated muscle forces using static optimization from over ground running data.

We analyzed the contributions of muscles to the ground reaction force and the resulting accelerations of the body mass center. Additional analyses, such as determining how muscles contribute to the flow of energy between body segments and joint accelerations, may provide a more comprehensive view of muscle actions during running. The results of any analysis depend on the musculoskeletal model (i.e., degrees of freedom, inertial parameters of body segments, muscle geometry, musculotendon parameters, etc.), the ground contact model, and the simulated muscle forces. We compared our simulated results to experimental measurements when possible (e.g., Fig. 2, Supplemental Figs. 1, 2, 6–8), and we verified that the sum of accelerations produced by all of the forces in the simulation was similar to the measured mass center acceleration (Supplemental Fig. 4). However, not all of the simulation results can be verified experimentally.

Musculoskeletal simulations provide a framework to examine quantities that are generally not measurable, such as muscle forces, and analyze how those quantities affect motion. In this study, we characterized how forces from muscles and arm swing affect dynamics of the body during running over a range of speeds by creating and analyzing muscle-driven simulations of ten male subjects running at four speeds. We have presented methods for generating these simulations with experimental data and rigorously examining the simulated output for accuracy. To enable others to

reproduce the results of our simulations and extend this work, all of the software, models, and data used to create and analyze the simulations are freely available. We provide open-access to the 120 subject-specific simulations developed for this study at simtk.org/home/nmbl_running for analysis in OpenSim (Delp et al., 2007). These simulations, and the associated musculoskeletal models and experimental data, provide a wealth of information to further examine the biomechanics of human running.

Conflicts of interest

None of the authors had any financial or personal conflict of interest with regard to this study.

Acknowledgments

Experimental data were collected at the Stanford Human Performance Lab. We would like to thank Edith Arnold, Matt DeMers, Amy Silder, Rebecca Shultz, and Phil Cutti for assistance with data collection; Ajay Seth, Ayman Habib, and Michael Sherman for technical support; and Tim Dorn, Melinda Cromie, Gabriel Sanchez, Ian Stavness, and Jack Wang for feedback on the manuscript. Samuel Hamner was supported by fellowships from Stanford University and the National Science Foundation. This work was also supported by the NIH Grants U54 GM072970, R24 HD065690, and R01 HD033929.

Appendix A. Supplementary information

Supplementary data associated with this article can be found in the online version at http://dx.doi.org/10.1016/j.jbiomech.2012.11.024.

References

Alexander, R.M., Bennet-Clark, H.C., 1977. Storage of elastic strain energy in muscle and other tissues. Nature 265, 114–117.
Anderson, F.C., Pandy, M.G., 1999. A dynamic optimization solution for vertical jumping in three dimensions. Computer Methods in Biomechanics and Biomedical Engineering 2, 201–231.
Besier, T.F., Fredericson, M., Gold, G.E., Beaupre, G.S., Delp, S.L., 2009. Knee muscle forces during walking and running in patellofemoral pain patients and pain-free controls. Journal of Biomechanics 42, 898–905.
Biewener, A.A., Roberts, T.J., 2000. Muscle and tendon contributions to force, work, and elastic energy savings: a comparative perspective. Exercise and Sport Sciences Reviews 28, 99–107.
Buchanan, T.S., Lloyd, D.G., Manal, K., Besier, T.F., 2005. Estimation of muscle forces and joint moments using a forward-inverse dynamics model. Medicine and Science in Sports and exercise 37, 1911–1916.
Cappellini, G., Ivanenko, Y.P., Poppele, R.E., Lacquaniti, F., 2006. Motor patterns in human walking and running. Journal of Neurophysiology 95, 3426–3437.
Cavagna, G.A., Franzetti, P., Heglund, N.C., Willems, P., 1988. The determinants of the step frequency in running, trotting and hopping in man and other vertebrates. Journal of Physiology 399, 81–92.
Cavagna, G.A., Thys, H., Zamboni, A., 1976. The sources of external work in level walking and running. Journal of Physiology 262, 639–657.
Cavanagh, P.R., Lafortune, M.A., 1980. Ground reaction forces in distance running. Journal of Biomechanics 13, 397–406.
Corcos, D.M., Gottlieb, G.L., Latash, M.L., Almeida, G.L., Agarwal, G.C., 1992. Electromechanical delay: an experimental artifact. Journal of Electromyography and Kinesiology 2, 59–68.
Delp, S.L., Anderson, F.C., Arnold, A.S., Loan, P., Habib, A., John, C.T., Guendelman, E., Thelen, D.G., 2007. OpenSim: open-source software to create and analyze dynamic simulations of movement. IEEE Transactions on Bio-medical Engineering 54, 1940–1950.
Delp, S.L., Loan, J.P., Hoy, M.G., Zajac, F.E., Topp, E.L., Rosen, J.M., 1990. An interactive graphics-based model of the lower extremity to study orthopaedic surgical procedures. IEEE Transactions on Bio-medical Engineering 37, 757–767.
Derrick, T.R., Hamill, J., Caldwell, G.E., 1998. Energy absorption of impacts during running at various stride lengths. Medicine and Science in Sports and Exercise 30, 128–135.
Dorn, T.W., Schache, A.G., Pandy, M.G., 2012. Muscular strategy shift in human running: dependence of running speed on hip and ankle muscle performance. Journal of Experimental Biology 215, 1944–1956.
Edgerton, V.R., Smith, J.L., Simpson, D.R., 1975. Muscle fibre type populations of human leg muscles. Histochemical Journal 7, 259–266.
Farris, D.J., Sawicki, G.S., 2012. Human medial gastrocnemius force-velocity behavior shifts with locomotion speed and gait. Proceedings of the National Academy of Sciences of the United States of America 109, 977–982.
Gamage, S.S., Lasenby, J., 2002. New least squares solutions for estimating the average centre of rotation and the axis of rotation. Journal of Biomechanics 35, 87–93.
Hamner, S.R., Seth, A., Delp, S.L., 2010. Muscle contributions to propulsion and support during running. Journal of Biomechanics 43, 2709–2716.
Hildebrand, M., 1960. How animals run. Scientific American 202, 148–157.
Hinrichs, R., Cavanagh, PR, Williams, KR, 1987. Upper extremity function in running I: center of mass and propulsion considerations. International Journal of Sport Biomechanics 3, 222–241.
Kuo, A.D., 1998. A least-squares estimation approach to improving the precision of inverse dynamics computations. Journal of Biomechanical Engineering 120, 148–159.
Lichtwark, G.A., Bougoulias, K., Wilson, A.M., 2007. Muscle fascicle and series elastic element length changes along the length of the human gastrocnemius during walking and running. Journal of Biomechanics 40, 157–164.
McClay, I., Lake, MJ, Cavanagh, PR, 1990. Muscle activity in running. In: Cavanagh, P.R. (Ed.), Biomechanics of Distance Running. Human Kinetics Books, Champaign, IL, pp. 165–186.
McMahon, T.A., Cheng, G.C., 1990. The mechanics of running: how does stiffness couple with speed? Journal of Biomechanics 23 (1), 65–78.
Mercer, J.A., Bezodis, N.E., Russell, M., Purdy, A., DeLion, D., 2005. Kinetic consequences of constraining running behavior. Journal of Sports Science and Medicine 4, 144–152.
Miller, R.H., Umberger, B.R., Caldwell, G.E., 2012a. Limitations to maximum sprinting speed imposed by muscle mechanical properties. Journal of Biomechanics 45, 1092–1097.
Miller, R.H., Umberger, B.R., Graham C.E., 2012b. Sensitivity of maximum sprinting speed to characteristic parameters of the muscle force–velocity relationship. Journal of Biomechanics 45, 1406–1413.
Nigg, B.M., De Boer, R.W., Fisher, V., 1995. A kinematic comparison of overground and treadmill running. Medicine and Science in Sports and Exercise 27, 98–105.
Novacheck, T.F., 1998. The biomechanics of running. Gait and Posture 7, 77–95.
Pontzer, H., Holloway, J.H., Raichlen, D.A., Lieberman, D.E., 2009. Control and function of arm swing in human walking and running. Journal of Experimental Biology 212, 523–534.
Robertson, D.G., Dowling, J.J., 2003. Design and responses of Butterworth and critically damped digital filters. Journal of Electromyography and Kinesiology 13, 569–573.
Sasaki, K., Neptune, R.R, 2006. Differences in muscle function during walking and running at the same speed. Journal of Biomechanics 39, 2005–2013.
Schache, A.G., Blanch, P.D., Dorn, T.W., Brown, N.A., Rosemond, D., Pandy, M.G., 2011. Effect of running speed on lower limb joint kinetics. Medicine and Science in Sports and exercise 43, 1260–1271.
Schache, A.G., Dorn, T.W., Blanch, P.D., Brown, N.A., Pandy, M.G., 2012. Mechanics of the human hamstring muscles during sprinting. Medicine and Science in Sports and Exercise 44, 647–658.
Swanson, S.C., Caldwell, G.E., 2000. An integrated biomechanical analysis of high speed incline and level treadmill running. Medicine and science in sports and exercise 32, 1146–1155.
Thelen, D.G., Anderson, F.C., 2006. Using computed muscle control to generate forward dynamic simulations of human walking from experimental data. Journal of Biomechanics 39, 1107–1115.
Thelen, D.G., Anderson, F.C., Delp, S.L., 2003. Generating dynamic simulations of movement using computed muscle control. Journal of Biomechanics 36, 321–328.
Wank, V., Frick, U., Schmidtbleicher, D., 1998. Kinematics and electromyography of lower limb muscles in overground and treadmill running. International Journal of Sports medicine 19, 455–461.
Weyand, P.G., Sternlight, D.B., Bellizzi, M.J., Wright, S., 2000. Faster top running speeds are achieved with greater ground forces not more rapid leg movements. Journal of Applied Physiology 89, 1991–1999.
Winter, D.A., 1983. Moments of force and mechanical power in jogging. Journal of Biomechanics 16, 91–97.
Winter, D.A., 1990. Biomechanics and Motor Control of Human Movement, 2nd ed. Wiley, New York.
Zajac, F.E., 1989. Muscle and tendon: properties, models, scaling, and application to biomechanics and motor control. Critical Reviews in Biomedical Engineering 17, 359–411.